

Galloping analysis of stranded electricity conductors in skew winds

J. H. G. Macdonald*, P. J. Griffiths and B. P. Curry

Department of Civil Engineering, University of Bristol, Queen's Building, University Walk, Bristol, UK
(Received February 20, 2007, Accepted June 23, 2008)

Abstract. When first commissioned, the 1.6 km span 275kV Severn Crossing Conductor experienced large amplitude vibrations in certain wind conditions, but without ice or rain, leading to flashover between the conductor phases. Wind tunnel tests undertaken at the time identified a major factor was the lift generated in the critical Reynolds number range in skew winds. Despite this insight, and although a practical solution was found by wrapping the cable to change the aerodynamic profile, there remained some uncertainty as to the detailed excitation mechanism. Recent work to address the problem of dry inclined cable galloping on cable-stayed bridges has led to a generalised quasi-steady galloping formulation, including effects of the 3D geometry and changes in the static force coefficients in the critical Reynolds number range. This generalised formulation has been applied to the case of the Severn Crossing Conductor, using data of the static drag and lift coefficients on a section of the stranded cable, from the original wind tunnel tests. Time history analysis has then been used to calculate the amplitudes of steady state vibrations for comparison with the full scale observations. Good agreement has been obtained between the analysis and the site observations, giving increased confidence in the applicability of the generalised galloping formulation and providing insight into the mechanism of galloping of yawed and stranded cables. Application to other cable geometries is also discussed.

Keywords: galloping; critical Reynolds number; yawed cable; stranded cable; transmission line; time history analysis.

1. Introduction

It is well known that electricity transmission lines can be prone to galloping due to accreted ice forming an aerodynamically unstable cross-section (Den Hartog 1956). Vibrations from this cause have often been observed in the field (e.g. Lilien, *et al.* 1998). However, this is just one form of a broader class of galloping instabilities, defined here as those which can be described using quasi-steady theory (i.e. purely in terms of the instantaneous relative velocity and the static force coefficients). The aim of this paper is to apply a new generalised galloping formulation to the case of galloping of un-iced stranded electricity conductors in skew winds, both to gain insight into the mechanism driving this form of galloping and to assess the validity of the formulation for potential wider application.

1.1. Generalised galloping analysis

Classical galloping, in one degree-of-freedom (1DOF) across wind, is covered by the well-known Den

* Corresponding Author, E-mail: John.Macdonald@bristol.ac.uk

Hartog criterion (1956). For bundled or iced electricity transmission lines, the rotational degree of freedom can also be important (Simpson 1983, Lilien, *et al.* 1998), but for single circular or spirally wound cables in the absence of ice or rain, rotations are not significant since they do not change the quasi-static aerodynamic forces. There is, however, potential coupling, through the aerodynamic forces, of translational vibrations in two orthogonal planes. This was first addressed by Jones (1992), although limited to winds normal to the cable axis and outside the critical Reynolds number range.

In more recent years there has been considerable interest in ‘dry inclined cable galloping’ of bridge stay-cables, in the absence of ice or rain. An explanation of this behaviour, put forward by Macdonald and Larose (2006), is that it is a consequence of changes in the static force coefficients in the critical Reynolds number range. As such, it can be considered using quasi-steady theory, but with the inclusion of three-dimensional and Reynolds number effects. This approach was extended to give a generalised galloping formulation for coupled vibrations in two translational degrees-of-freedom (2DOF) (Macdonald and Larose 2008a). Solutions were given for the level of structural damping required to prevent the galloping, for both perfectly tuned and detuned natural frequencies in the two planes (Macdonald and Larose 2008a, 2008b). Meanwhile, Carassale, *et al.* (2005) developed a similar 2DOF quasi-steady model of galloping, although they chose not to include changes of the force coefficients with Reynolds number in their formulation.

It is suggested that the generalised galloping analysis (Macdonald and Larose 2008a) can be applied to any form of galloping where rotations are not significant, including the present case of galloping of stranded electricity transmission lines in skew winds. This will be assessed by application of the method to a well documented case study of a stranded conductor which exhibited large amplitude vibrations.

1.2. Case study: Severn Crossing Conductor

The Severn Crossing Conductor is a set of six 275kV electrical cables (plus one earth cable) spanning 1620 m across the Severn Estuary between England and Wales, at an elevation of up to 150 m, just downstream of the Severn Bridge (Fig. 1). When the crossing was commissioned in 1959, numerous electrical faults occurred due to flashovers between the cables spaced vertically 8.2 m apart. Oscillations, primarily of the first anti-symmetric mode shape (i.e. full sine wave) in each plane, and occasionally of the first symmetric mode in each plane, were observed (Davis, *et al.* 1963). This is consistent with classical galloping, for which the first anti-symmetric mode is normally the most troublesome (Simpson 1983). However, no ice or rain was present, so the behaviour could not be explained by classical galloping theory.

The winds causing the large oscillations were from a direction at approximately 70° to the transmission line axis. Winds from this direction blow over a long fetch of open water, so typically have a low turbulence intensity.

Each cable was made up of a central strand and five inner layers of steel strands (91 total) and two outer layers of aluminium wires (78 total), each 2.87 mm in diameter (Davis, *et al.* 1963). The outside layer had 42 circular strands, wound in a 17° pitch angle right-handed helix (Counihan 1963), and the overall diameter was 43 mm (strand:diameter ratio 1:15). The total cross-sectional area was 1090 mm², the measured effective modulus of elasticity 117×10^9 N/m², the total mass per unit length 6.40 kg/m (including grease), and the nominal horizontal tension 270kN.

Wind tunnel tests were undertaken to determine the static drag and lift forces on the cable as a function of wind speed and direction, initially at the former National Physical Laboratory, Teddington



Fig. 1 Severn Crossing Conductor and Severn Bridge

(Gould and Lawes 1960) and at the University of Bristol (Sewell and Taylor 1961), then more comprehensively at Imperial College, London (Counihan 1963). A full account of the aerodynamic investigations is given by Richards (1963). It was concluded that the vibrations were due to a form of galloping related to the lift force generated in the critical Reynolds number range (corresponding to wind speeds of around 13 m/s), due to the different effective orientations of the helically wound strands on the upper and lower surfaces of the cable in skew winds (Davis, *et al.* 1963). However, the details of the excitation mechanism were not clear. Subsequent smoothing of the cables profiles was undertaken by wrapping them with PVC tape and this was successful in eliminating further oscillations. The conductors were eventually replaced by smooth (interlocking trapezoidal) stranded cables (Simpson 1983).

The galloping behaviour was partially explained by Simpson (1965), considering variation of the drag and lift forces with wind velocity. It was suggested that the primary mechanism was along-wind (horizontal) excitation due to the negative slope of the drag-force/velocity curve (i.e. the drag crisis), which, for finite slope of the lift-force/velocity curve, could cause vertical excitation of the cable as a secondary effect. The new generalised galloping formulation now allows the behaviour to be re-analysed, to give further insight into the mechanism and to relate it to other forms of galloping. Also, advances in computing power now allow much more extensive numerical analysis, to cover the full parameter range of the available data and to calculate steady state amplitudes through time history analysis.

2. Preliminary data and analysis

2.1. Wind tunnel data

The original Imperial College wind tunnel data (Counihan 1963, Davis, *et al.* 1963, Richards 1963) provide values for the drag and lift force coefficients for wind speeds of 6-20m/s and directions of 67.5-90°, relative to the cable axis. These data are reproduced in Fig. 2 (a wind speed of 10 m/s is equivalent to a Reynolds number of 2.9×10^4). The wind speed range covers the critical Reynolds number region.

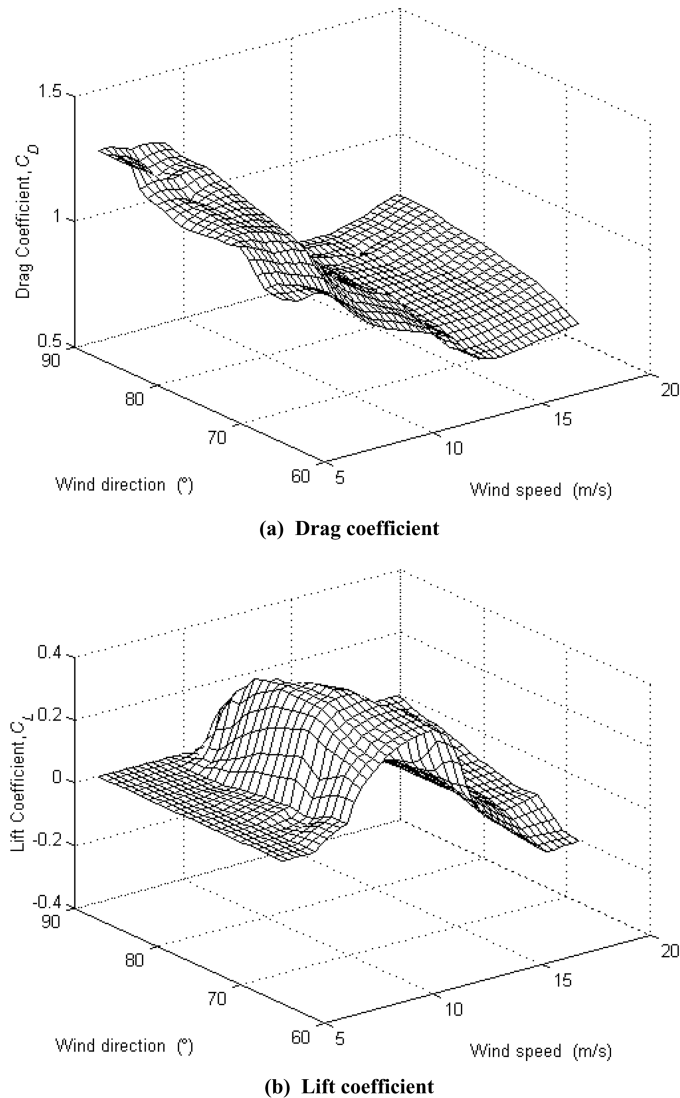


Fig. 2 Force coefficient data from original Imperial College wind tunnel tests (Counihan 1963, Davis, *et al.* 1963, Richards 1963)

As well as the characteristic drop in drag coefficient with increasing wind speed, it is clear that significant lift is generated within this range for skew winds, although not for wind normal to the cable.

The critical Reynolds number is approximately 4×10^4 , which is an order of magnitude lower than for a smooth circular cylinder in smooth flow (ESDU 1986). Hence the corresponding critical wind speed is not very high, despite the relatively small diameter of the cable. The behaviour is in some ways similar to a rough circular cylinder, but Davis, *et al.* (1963) and Richards (1963) explain that there is separation and reattachment of the flow over each strand, causing some differences, including a greater reduction in the drag coefficient.

The lift is generated by asymmetry of the final separation points. In skew winds, the strands on one side of the cable are more nearly aligned with the flow than on the other, giving a 'smooth' and

a ‘rough’ side. The transition to a turbulent boundary layer occurs at lower Reynolds number on the rough side than the smooth side, which causes delayed final separation and hence a net lift force directed towards the rough side in the critical Reynolds number range (Davis, *et al.* 1963, Richards 1963). The maximum lift occurred for a skew angle approximately equal to the helix pitch angle (i.e. for wind normal to the strands on the rough side).

2.2. Static equilibrium configuration

Before addressing the dynamic behaviour of the conductor, it is necessary to consider its static equilibrium configuration allowing for the static wind loads.

For the purpose of this analysis, the axis of the conductor is taken to be horizontal. Considering gravity loading, the actual maximum inclination at the ends of the span is 11° , which for the maximum skew angle considered (67.5°), makes less than 0.5° difference to the cable-wind angle compared with the horizontal cable assumption.

For a uniform horizontal wind, the sway angle of the static equilibrium cable plane relative to the vertical plane is given by:

$$\theta = \arctan\left(\frac{F_D}{mg - F_L}\right) \quad (1)$$

where m is the cable mass per unit length, g the acceleration due to gravity, and F_D and F_L are the static drag and lift forces respectively, per unit length.

Using the measured static force coefficients, the calculated sway angles are given in Fig. 3. It can be seen that the sway angle is around 3° in the critical Reynolds number range.

3. Linearised galloping analysis

Having defined the static equilibrium configuration of the cable, its potential for galloping is

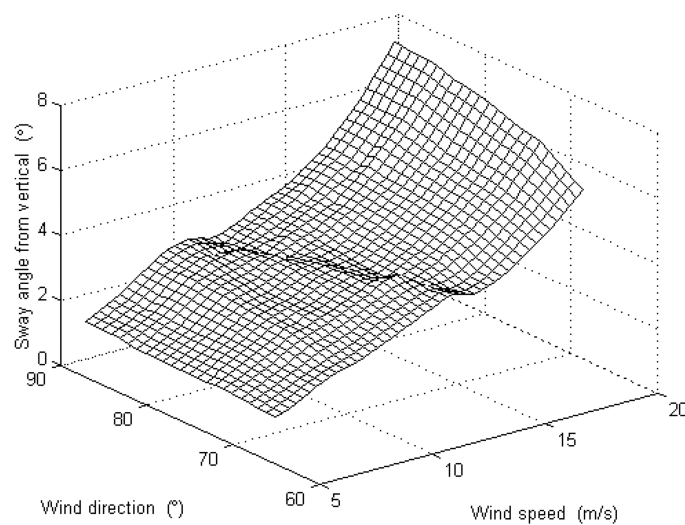


Fig. 3 Sway angle from vertical due to static wind loading

assessed. Firstly linearised galloping analysis is used to consider the dynamic stability of small vibrations. The above force coefficient data have been substituted into the generalised quasi-steady galloping formulation (Macdonald and Larose 2006, 2008a, 2008b). It can be argued that quasi-steady theory is applicable in the present situation since around the critical Reynolds number the reduced velocity of the first few modes is of the order of 1000, indicating that the time scale for structural vibrations is far longer than for flow effects, so quasi-steady flow conditions are very likely to have time to develop throughout the vibration cycle.

For cables with sag, the natural frequencies of the in-plane symmetric modes, particularly the first, are increased relative to the solution for a taut string, which applies to all other modes of fixed-ended cables (Irvine 1981). For the Severn Conductor, based on the nominal cable parameters (Section 1.2), Irvine's non-dimensional sag parameter (λ^2) is 66, giving a natural frequency of the first symmetric in-plane mode shape (modified half sine wave) of 0.149Hz (period 6.7s), 2.4 times the first symmetric out-of-plane natural frequency of 0.063Hz (period 15.8s). Hence, the first symmetric in-plane and out-of-plane modes are sufficiently separated in frequency to be treated as essentially single-degree-of-freedom (1DOF) cases (Macdonald and Larose 2008b). This is considered in the following section 3.1. For anti-symmetric modes and higher symmetric modes, the in-plane and out-of-plane natural frequencies are almost coincident. For the Severn Conductor the natural frequencies of the first anti-symmetric in-plane and out-of-plane modes (full sine wave) are approximately equal, at a frequency of 0.127Hz (period 7.9s). For equal (or close) natural frequencies, modal coupling becomes important and each mode pair needs to be considered for two-degree-of-freedom (2DOF) galloping (Macdonald and Larose 2008a), which is addressed in Section 3.1.

3.1. Single-degree-of-freedom galloping

Full details of the mechanism and derivation of the equations for 1DOF galloping are given by Macdonald and Larose (2006), but they are briefly covered here.

For vibrations in a given plane, the component of the quasi-steady aerodynamic force, per unit length, acting in the direction of motion is given by:

$$F_x = \frac{1}{2} \rho U_R^2 D (C_D \cos \alpha_R - C_L \sin \alpha_R) \quad (2)$$

where ρ is the fluid density, U_R is the magnitude of the relative velocity, D is the cable diameter, α_R is the relative angle of attack, and C_D and C_L are the drag and lift coefficients respectively.

This force is a function of the cable velocity, \dot{x} , through the relative velocity, the resulting changes in the force coefficients, and the angle α_R . It therefore effectively provides a non-linear damping term in the equation of motion of the cable. For small amplitude vibrations in a given mode, the equivalent linear aerodynamic damping ratio is given by:

$$\zeta_a = \frac{-1}{4\pi m f_n} \left. \frac{dF_x}{d\dot{x}} \right|_{\dot{x}=0} \quad (3)$$

where f_n is the natural frequency.

Differentiating Eq. (2) (for the general case of three-dimensional geometry and variable force coefficients) and substituting into Eq. (3), yields a general expression for the aerodynamic damping ratio ζ_a , which can be negative, causing galloping. Hence, the minimum structural damping required to

prevent 1DOF galloping, for circular or spirally stranded cables, for which $\partial C_D/\partial \alpha = \partial C_L/\partial \alpha = 0$, is given by (Macdonald and Larose 2006, 2008a):

$$Z_s \equiv \frac{mf_n \zeta_s}{\mu} > \frac{-\text{Re}}{8\pi} \left[g(C_D) \cos^2 \alpha - g(C_L) \sin \alpha \cos \alpha + \frac{C_D}{\sin \phi} \right] \quad (4)$$

where, $g(C_F) = C_F \left(2 \sin \phi - \frac{1}{\sin \phi} \right) + \frac{\partial C_F}{\partial \text{Re}} \text{Re} \sin \phi + \frac{\partial C_F}{\partial \phi} \cos \phi$, $C_F = C_D$ or C_L ,

ζ_s is the structural damping ratio, μ is the dynamic (absolute) fluid viscosity, α is the angle of attack in the plane normal to the cable axis (in this case the vertical angle of attack), ϕ is the angle between the wind velocity and the cable axis (in this case the wind direction relative to the cable axis, in the horizontal plane), and $\text{Re} = \rho DU/\mu$ is the Reynolds number, where U is the mean wind speed.

Considering the static equilibrium configuration (Section 2.2), the angle of attack (α) for in-plane modes is $90^\circ - \theta$, and for out-of-plane modes is $-\theta$.

Substituting the measured force coefficient data and the basic cable parameters for the Severn Crossing Conductor into Eq. (4) yields solutions for the minimum structural damping required to prevent 1DOF galloping in the first symmetric in-plane and out-of-plane modes, shown in Fig. 4 (for the full range of wind speeds and directions tested in the wind tunnel). Where the solution is negative, galloping would not occur even in the absence of any structural damping.

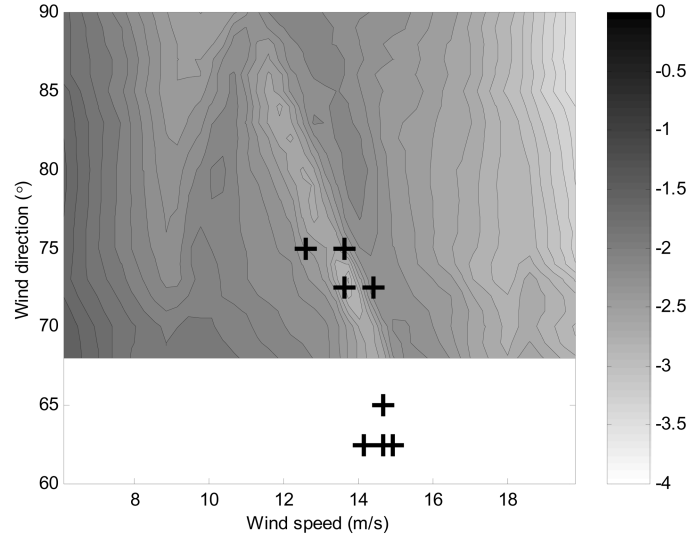
On this basis, the first symmetric in-plane mode was not found to be prone to galloping (Fig. 4(a)). The in-plane behaviour is dominated by the C_D term, which is always beneficial, providing positive aerodynamic damping.

In contrast, a galloping instability was predicted for the first symmetric out-of-plane mode in the critical Reynolds number range, as shown by the positive damping requirement in the area bounded by the bold lines in Fig. 4(b). An instability exists for the full range of wind directions considered, including for wind normal to the cable. This behaviour is primarily due to the negative $\partial C_D/\partial \text{Re}$ term, i.e. the along-wind drag crisis. If sufficiently negative this leads to a negative gradient of the force/relative velocity graph, so along-wind cable motions lead to changes in the force which reinforce the motion.

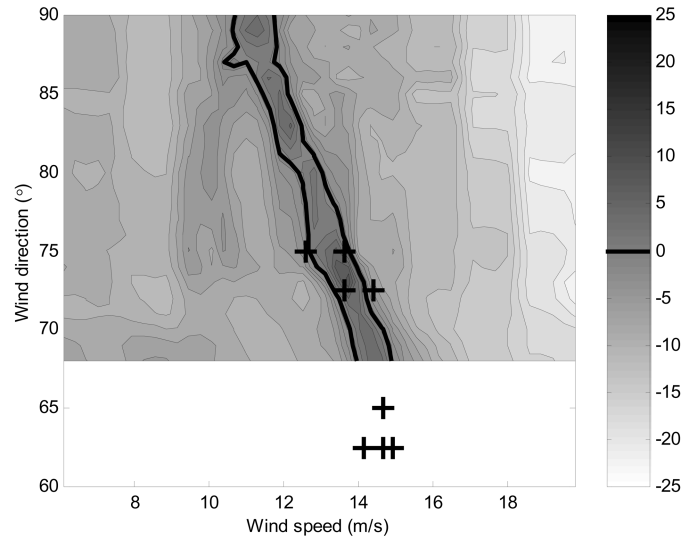
The crosses in Fig. 4 and subsequent figures indicate the wind conditions under which flashovers between the conductors were observed on site (Davis, *et al.* 1963). The wind data are averaged between the two anemometers used, with a mean elevation of 88 m, similar to the mean elevation of the cable (approximately 95 m). The accuracy of the averaged wind measurements is estimated to be 0.5 m/s in speed and 5° in direction. Unfortunately some observations of galloping on site were outside the range of wind directions for which force coefficient data are available from the wind tunnel tests. Nevertheless, there is good agreement between the site observations and the predicted conditions for galloping to occur for wind around 14 m/s at 73° . However, although vibrations in the first symmetric out-of-plane mode were sometimes observed on site (Davis, *et al.* 1963), vibrations in this mode would be close to horizontal. No flashover occurred between conductors spaced in this direction (12.8 m apart) and this analysis would not explain the flashovers that did occur on site between conductors spaced vertically apart.

3.2. Two-degree-of-freedom galloping

The above approach has been extended to deal with coupled vibrations in two orthogonal planes



(a) First symmetric in-plane mode (period 6.7s)



(b) First symmetric out-of-plane mode (period 15.8s)

Fig. 4 Structural damping (%) required to prevent 1DOF galloping in first symmetric in-plane and out-of-plane modes

(Macdonald and Larose 2008a), by defining the generalised aerodynamic damping matrix:

$$\mathbf{C}_a = - \begin{bmatrix} \frac{\partial F_x}{\partial \dot{x}} & \frac{\partial F_x}{\partial \dot{y}} \\ \frac{\partial F_y}{\partial \dot{x}} & \frac{\partial F_y}{\partial \dot{y}} \end{bmatrix}_{\dot{x}=\dot{y}=0} \quad (5)$$

where F_y and \dot{y} are the aerodynamic force and cable velocity in the direction orthogonal to x .

Considering Eq. (2) and the equivalent expression for F_y , this can then be expressed in terms of Re , α , ϕ and the force coefficients and their gradients. The total damping matrix is given by the sum of the aerodynamic damping matrix and the structural damping matrix:

$$\mathbf{C}_s = \begin{bmatrix} 4\pi m f_x \zeta_s & 0 \\ 0 & 4\pi m f_y \zeta_s \end{bmatrix} \quad (6)$$

where f_x and f_y are the natural frequencies in the two planes.

For the special case of perfectly tuned modes ($f_x = f_y = f_n$), the 2DOF complex eigenvalue problem has been solved analytically, giving the following non-dimensional solution for the minimum structural damping required to prevent galloping, for circular or spirally stranded cables (Macdonald and Larose 2008a):

$$Z_s \equiv \frac{m f_n \zeta_s}{\mu} > \mathcal{R} \left[\frac{\text{Re}}{16\pi} \left\{ -h(C_D) + \sqrt{g^2(C_D) + g^2(C_L) + h^2(C_L)} \right\} \right] \quad (7)$$

where $h(C_F) = g(C_F) + \frac{2C_F}{\sin \phi}$ and $\mathcal{R}[\]$ indicates the real part¹⁾.

Note that because of the perfect tuning in the orthogonal planes, this is now independent of the angle of attack or the static sway angle.

This formulation has recently been extended to include effects of wind turbulence (Symes and Macdonald 2007), but it is believed that for low turbulence intensities it has relatively little effect for stranded, rather than circular, cables (ESDU 1986). This assertion is supported for the Severn Conductor by the good correlation of measured force coefficients in the different wind tunnels used, despite their different turbulence characteristics (Richards 1963). Therefore, the modifications for the effects of turbulence are not included here.

Substituting the force coefficient data for the Severn Crossing Conductor into Eq. (7) yields the solutions shown in Fig. 5 for the first anti-symmetric mode pair. In the area of positive values, bounded by the bold line, the cable is prone to 2DOF galloping if insufficient structural damping is provided. There is good agreement with the site measurements of the wind conditions required to cause galloping, particularly considering the limited accuracy of the site measurements.

Considering the main factors affecting the structural damping requirement to prevent galloping, C_D is always a significant beneficial effect, providing positive aerodynamic damping. A galloping-type instability can occur for negative $g(C_D)$, but this can generally only occur if $\partial C_D / \partial \text{Re}$ is negative (i.e. the along-wind drag crisis). This is more significant at higher Re , due to the overall factor of Re in Eq. (7), so galloping is more likely, or requires a higher structural damping ratio to prevent it, at the upper end of the critical Reynolds number range. Expanding Eq. (7), it can be found that the other principal detrimental effect is if $C_L g(C_L)$ is negative, which generally only occurs when $C_L \partial C_L / \partial \text{Re}$ is negative, i.e. when the magnitude of C_L is reducing with increasing Re . The physical significance of this is that vibrations in an inclined plane have a component of velocity in the along-wind direction, causing a change in the relative Reynolds number and hence a change in the lift force. If this change in lift force is in the same direction as the vertical component of the

¹⁾ In fact each of the individual terms is real. This notation is used only to discount the square root if the expression under it is negative.

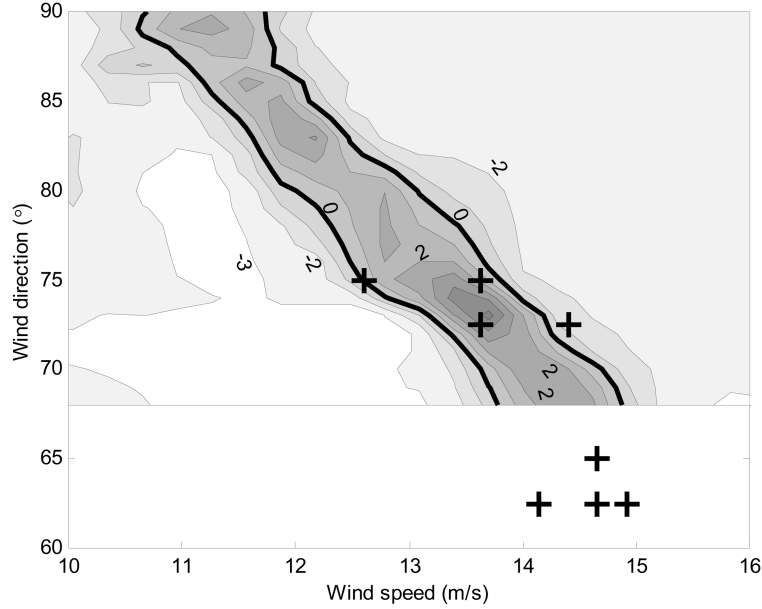


Fig. 5 Structural damping (%) required to prevent 2DOF galloping of the first anti-symmetric mode pair (period 7.9s)

velocity, the motion is enhanced.

Although the magnitude of C_L is significant over quite a wide range of wind speeds in the critical Reynolds number range ($9 \text{ m/s} < U < 15 \text{ m/s}$), and indeed C_L with the opposite sign exists at higher wind speeds (Fig. 2), for the range of wind speeds tested, $C_L \cdot \partial C_L / \partial \text{Re}$ is only negative in a narrow range of U and ϕ , which corresponds very closely to the area of aerodynamic instability shown in Fig. 5. The agreement with the site observations of galloping with this narrow range of wind velocities, rather than the wider range of wind velocities corresponding to the full critical Reynolds number range, suggests that the analysis properly describes the origin of the instability.

It is apparent from the definition of Z_s in Eqs. (4) and (7) that higher frequency modes require less structural damping, so for 2DOF galloping the first anti-symmetric mode pair is the most critical, which is again consistent with the site observations.

The cable trajectory at the onset of vibrations can also be found from the eigenvalue analysis. In general the eigenvectors are complex, indicating elliptical motion, but for perfectly tuned natural frequencies in the two planes they are normally real so the trajectory is planar, inclined at an angle relative to the horizontal given by (Macdonald and Larose 2008a):

$$\alpha_{resp0} = \arctan \left(\frac{g(C_D) + \sqrt{g^2(C_D) + g^2(C_L) - h^2(C_L)}}{h(C_L) - g(C_L)} \right) \quad (8)$$

Using the measured force coefficients, the calculated inclination angles are shown in Fig. 6. The bold lines indicate the boundaries of the area of galloping instability, from Fig. 5. For $\phi = 90^\circ$, the vibration plane is effectively horizontal (i.e. along-wind, dominated by the drag crisis), but for wind directions more than a few degrees from normal to the cable, the vibration plane is generally

inclined at around 60° to the horizontal (i.e. lift is more significant). For $\phi > 90^\circ$, the behaviour is symmetrical about $\phi = 90^\circ$, except the sign of the vibration plane inclination angle is reversed.

A special case of a ‘complex response’ can occur if the expression under the square root in Eqs. (7) & (8) is negative (Macdonald and Larose 2008a). This theoretically gives a two-dimensional ‘beating’ response, as first described by Jones (1992). However, for this to give divergent amplitude vibrations it also requires the structural damping demand to be positive. In practice the appropriate combination of conditions only generally occurs when $\partial C_D/\partial Re$ is negative and C_L is large or $C_L \cdot \partial C_L/\partial Re$ is positive. Hence it would tend to occur at the lower end of the critical Reynolds number range, whereas it is the higher end which is more likely to give galloping, as described above. Therefore, for the cable geometry considered, and probably most other cables, these complex responses are not of practical relevance and any 2DOF galloping responses of the perfectly tuned system are always planar, at least at their onset.

4. Time history analysis

The above analysis was able to predict the conditions under which galloping would be initiated, but it cannot predict the resulting vibration amplitudes. A time history analysis was therefore conducted, using the instantaneous relative velocity to give the aerodynamic forces at each time step. This could capture the non-linearity of the aerodynamic forces for large amplitude vibrations, and could hence find the steady state amplitude. However, it is still fundamentally based on quasi-steady theory.

In this analysis, it is assumed that the non-linearities of the aerodynamic forces dominate over any dynamic geometric non-linearities of the cable, so the structural vibration modes are taken to be linear about the static equilibrium configuration. Subsequently this assumption was tested by running a geometric non-linear analysis of the cable for the wind conditions giving the largest amplitude response. The maximum response was reduced by only 1.4%, indicating that indeed the

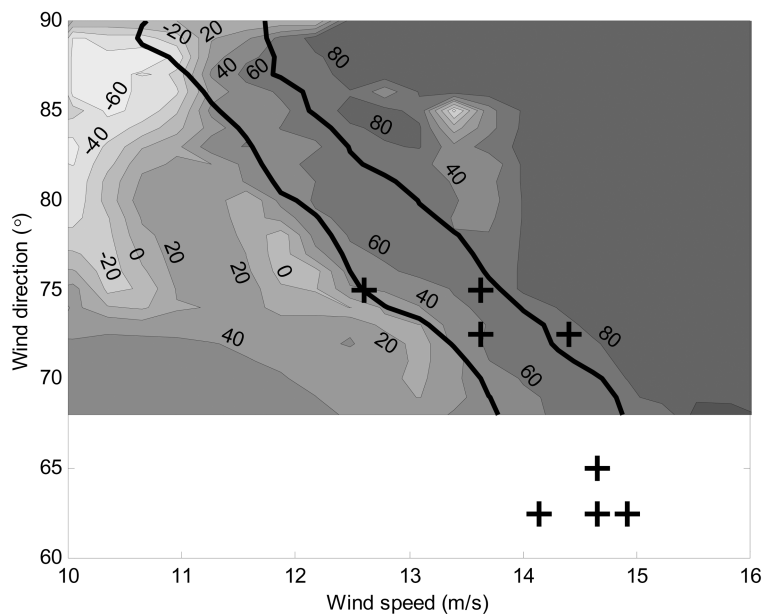


Fig. 6 Inclination ($^\circ$) of vibration plane from horizontal, from linearised galloping analysis

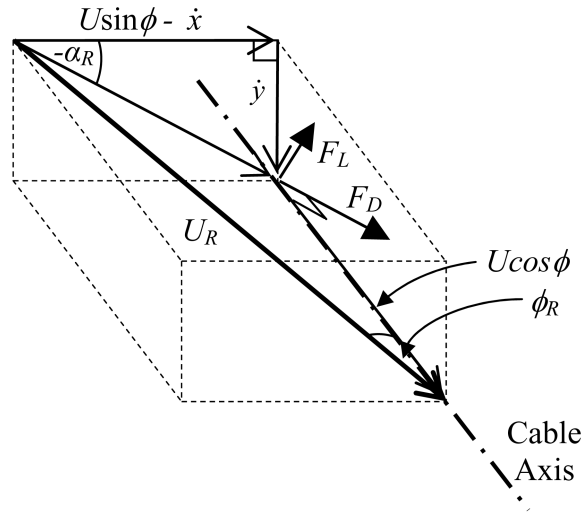


Fig. 7 3D view showing relative velocity and orientations of drag and lift force

aerodynamic non-linearities are dominant.

The instantaneous aerodynamic forces are considered when the cable has a local velocity with horizontal and vertical components \dot{x} and \dot{y} (Fig. 7). The forces are a function of the magnitude of the relative velocity (U_R) and the drag and lift coefficients, which are in turn functions of the relative Reynolds number (based on U_R) and relative cable-wind angle (ϕ_R). The forces are resolved into the x and y directions considering the relative angle of attack in the plane normal to the cable axis, α_R (Fig. 7). The static wind forces for no cable motion are subtracted to only consider the dynamic behaviour about the static equilibrium position.

Buffeting from wind turbulence would modify the actual responses, but for simplicity it is neglected in the analysis to concentrate on the aeroelastic instability itself. This would give a first approximation to the actual cable responses. It was subsequently estimated that for the maximum cable response the root mean square (RMS) cable velocity is more than three times the expected RMS wind velocity fluctuations for wind along the estuary.

The structural damping of long cables is very low (typically $< 0.1\%$), so for the purpose of this analysis it was taken to be zero. Subsequent checks found that 0.1% damping typically causes a 5% reduction in the predicted response amplitudes and 1% damping typically leads to a 40% reduction.

The generalised equations of motion were solved numerically as a time history analysis, using the MATLAB ordinary differential equation solver *ode45*, based on an explicit Runge-Kutta (4, 5) formula (Mathworks Inc. 2005). At each time step the generalised force of each mode was found by numerically integrating over the cable mode shapes using 24 elements along the cable, and the values of C_D and C_L were interpolated at each position, based on the instantaneous local relative velocity (U_R and ϕ_R). Small initial displacements from the equilibrium position were used to initiate vibrations. It was found that the solution normally converged on steady state vibrations (or a static solution) within 10 minutes (approximately 75 vibration cycles in the first anti-symmetric mode).

4.1. Two-degree-of-freedom galloping of perfectly tuned modes

Since the linearised analysis found that the first anti-symmetric mode pair was critical for 2DOF

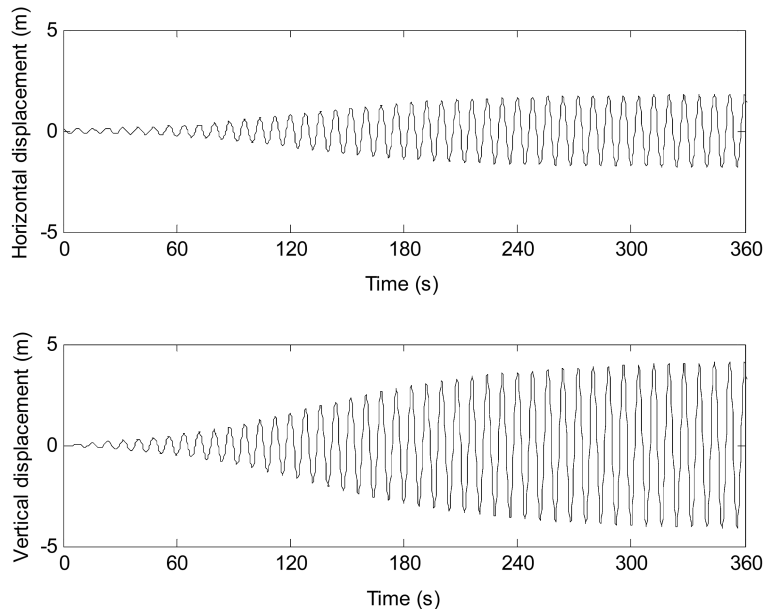


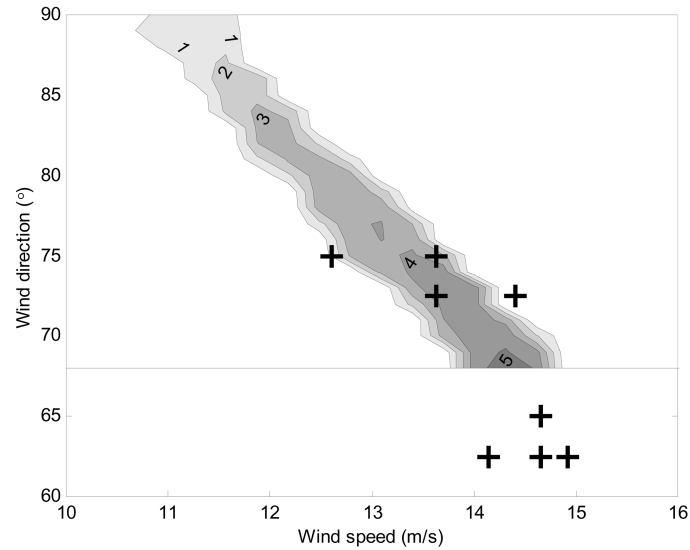
Fig. 8 Typical output of 2DOF time history analysis – response at antinode (first anti-symmetric mode pair, $U = 14$ m/s, $\phi = 70^\circ$)

galloping (Section 3.2), initially just this mode pair was included in the time history analysis. A typical solution, for particular wind conditions, is shown in Fig. 8.

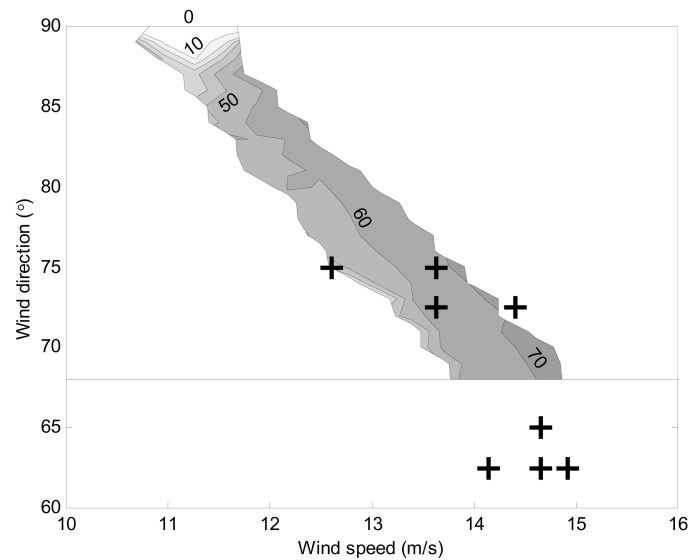
Where large amplitude steady state vibrations occurred, they were always found to be planar, which is consistent with the behaviour at the onset of vibrations from the linearised analysis (Section 3.2). The steady state vibration amplitudes and the orientations of the vibration planes are shown in Fig. 9. For very small initial displacements, the range of wind conditions for the instability to occur was found to be identical to that from the linearised analysis (Fig. 5), as expected. However, for large initial displacements, potentially caused by other excitation mechanisms, galloping can occur over a wider range of wind conditions, due to the non-linearity. Nevertheless, the linearised analysis does cover the worst case for the structural damping required to prevent galloping.

For wind normal to the cable, the steady state vibrations are horizontal (along-wind), with amplitudes up to 1.9 m, due to the drag crisis. But for wind directions more than a few degrees from 90° , the lift becomes important and the vibration plane increases in inclination, typically being around 60° from the horizontal (Fig. 9(b)), which is similar to the values from the linearised analysis at the onset of vibrations (Fig. 6). There is also a trend for larger amplitude vibrations at skew angles further from 90° and slightly higher wind speeds. The wind conditions for the observed galloping on site, shown as crosses in Fig. 9, are all quite close to an area where amplitudes in excess of 4 m were predicted. The maximum calculated response was 5.0 m vertical and 2.0 m horizontal, which agrees well with the one estimate of full-scale amplitudes of 5.5 m vertical and 1.2 m horizontal, with a period of 7.9s, i.e. in the first anti-symmetric mode in each plane (Davis, *et al.* 1963).

Considering 2DOF galloping in higher perfectly tuned mode pairs, the responses were identical except the amplitudes were inversely proportional to natural frequency, since it is the cable velocity



(a) Amplitude at antinode (m)



(b) Inclination of vibration plane from horizontal (°)

Fig. 9 Amplitude and orientation of steady state vibrations from 2DOF time history analysis (first anti-symmetric mode pair)

that dictates the behaviour.

4.2. Detuned and multiple-degree-of-freedom galloping

Further time history analysis was undertaken to consider the responses of detuned pairs of modes and combinations of several modes. For detuned natural frequencies it was necessary to consider the modal vibration planes orientated in the swayed equilibrium configuration (Section 2.2).

Simpson (1965) gives calculated natural frequencies of the first anti-symmetric in-plane and out-of-plane modes which are actually detuned by 1.3% due to coupling with the adjacent spans. 2DOF time history analysis of this slightly detuned system gave very similar responses as for the perfectly tuned system, but with the cable trajectory being elliptical, as shown, for example, in Fig. 10.

The symmetric in-plane modes, particularly the lowest modes, have elevated natural frequencies relative to the corresponding out-of-plane modes, due to the sag, giving much greater detuning. Also, the mode shapes are modified from the otherwise sinusoidal shapes. On this basis, 2DOF time history analysis of the first symmetric in-plane and out-of-plane modes showed very little response in-plane, but effectively 1DOF galloping out-of-plane. This was consistent with the 1DOF linearised analysis in each plane (Section 3.1, Fig. 4), since the natural frequencies are well separated so the coupling is minor. The maximum out-of-plane amplitude was 3.72 m for a wind of 11.3m/s at 90° to the cable, i.e. twice the 2DOF first anti-symmetric mode response in the same wind conditions. For skewed winds the out-of-plane first symmetric mode response was somewhat less than for the first anti-symmetric mode pair, since, despite the lower natural frequency, it was effectively limited to the one plane and was driven primarily by the drag crisis, with minimal effect of the lift.

In a multi-mode analysis considering the first six modes in each plane, the symmetric in-plane modes tended to decay, effectively each behaving as an independent stable 1DOF system, due to the detuning. However, all other modes have commensurate natural frequencies and had previously been found to exhibit 1DOF or 2DOF galloping, so there was more opportunity for multiple-degree-of-freedom (MDOF) responses.

Considerable variation in the MDOF responses were found depending on the wind conditions and initial conditions specified, but the following general observations were made. Except for winds close

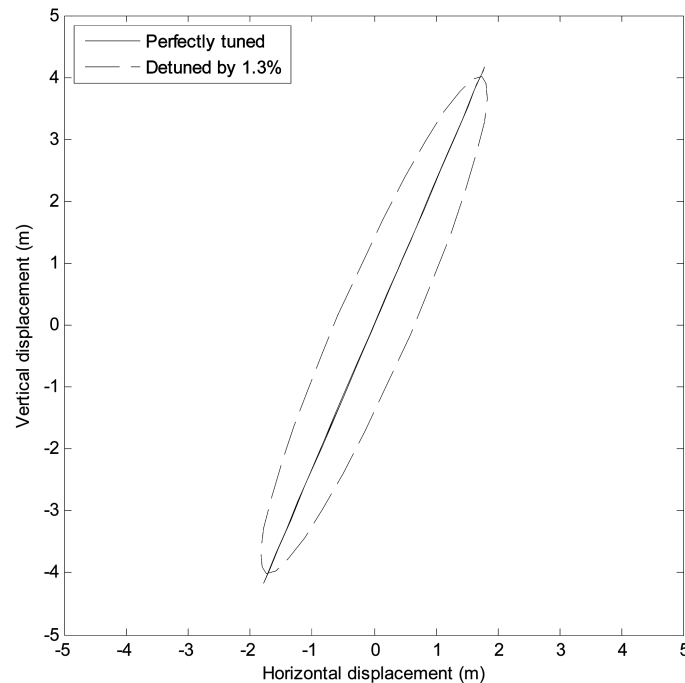


Fig. 10 Steady state trajectory of antinode of first anti-symmetric mode pair for perfectly tuned and slightly detuned natural frequencies ($U = 14$ m/s, $\phi = 70^\circ$)

to normal to the cable, out-of-plane symmetric modes tended to decay in favour of anti-symmetric mode pairs. The steady state most often tended towards the 2DOF first anti-symmetric mode pair solution. However, for larger initial velocities in other anti-symmetric modes, they could become dominant, again acting as 2DOF pairs. Equal damping in all modes, even as low as 0.1%, tended to increase the dominance of the first anti-symmetric mode pair and reduce the time for other modes to decay. This is because the structural damping coefficients (Eq. (6)) are proportional to natural frequency, but the aerodynamic damping matrix (Eq. (5)) is independent of natural frequency. For wind normal to the cable (i.e. drag crisis excitation), in-plane modes decay rapidly and, in the absence of structural damping, all out-of-plane modes grow at the same rate with time, since the effective aerodynamic damping coefficient is the same. In this case, generally the mode with the highest velocity amplitude becomes dominant, although again it depends on the initial conditions.

Hence, overall there is considerable complexity of the MDOF behaviour and it is dependent on the actual wind conditions and initial conditions. This is consistent with the site observations, where each of the seven conductors (nominally identical) often responded quite differently from each other (Davis, *et al.* 1963). However, from the analysis, the most likely and largest amplitude galloping response is 2DOF galloping of the first anti-symmetric mode pair, as in Sections 3.2 and 4.1, which agrees with the site observations of the behaviour leading to flashover between the conductors (Davis, *et al.* 1963). Although the predicted steady state vibration planes are inclined, wind buffeting and contributions from other modes could lead the vertically spaced conductors to come close enough for flashover to occur.

5. Application to other cable geometries

Full application of the generalised galloping analysis requires wind tunnel data of the drag and lift coefficients as functions of both Reynolds number and cable-wind angle (and angle of attack, where relevant). Unfortunately such extensive data are available for very few cable geometries.

Apart from the Severn Conductor cable geometry itself, with 42 outer strands, Counihan (1963) performed wind tunnel tests on similar cables with 24 and 18 outer strands (strand:diameter ratios 1:9 and 1:7 respectively). They exhibited qualitatively similar behaviour in the critical Reynolds number range, but the transitions were less severe. The drop in drag coefficient from sub-critical to super-critical Reynolds numbers was 50% for the 42 strand cable, 33% for the 24 strand cable and 25% for the 18 strand cable, for zero yaw. The maximum lift coefficients for the three cables were 0.34, 0.12 and 0.08 respectively, and the drop in the lift coefficient at the upper edge of the critical Reynolds number range was more gradual for the cables with fewer outer strands.

The generalised galloping analysis was applied to the data for the 24 and 18 strand cables, yielding similar patterns as for the 42 strand cable, but with no galloping. The 24 strand cable was just stable and the 18 strand cable was considerably more stable. The major factor was that the magnitude of the potentially detrimental term in $C_L \cdot \partial C_L / \partial \text{Re}$ was greatly reduced, since it is approximately proportional to the maximum value of C_L squared. Also $\partial C_D / \partial \text{Re}$ was insufficiently negative to cause along-wind vibrations.

Nebres, *et al.* (1993) discuss the wide variety of potential cable geometries and present drag and lift coefficients for a few cable geometries with up to 12 outer strands (strand:diameter ratio 1:5). Their tests were conducted for Reynolds numbers from 6.0×10^3 to 4.6×10^4 , but it was identified that the flow regime was always sub-critical (Nebres and Batill 1992). They conclude that, whereas cables with 12 or more outer strands behave similarly to a circular cylinder (though see Section

2.1), those with up to 6 outer strands have a different behaviour. For these cables the lift is directed towards the smooth side – the opposite to the 42 strand cable in the critical Reynolds number range (Section 2.1). The explanation given is that on the smooth side there is a lower adverse pressure gradient for the flow over each strand than on the rough side, giving delayed separation.

Unfortunately, the data from Nebres, *et al.* (1993), at a few discrete values of Reynolds number (Re) and cable-wind angle (ϕ), are rather sparse for reliable application of the generalised galloping analysis, for which the gradients of the force coefficients with Re and ϕ are important. Nevertheless, the data show that there is little dependence on Re , so it seems unlikely that these cables would exhibit galloping, at least within the range of Reynolds numbers tested.

For the Severn Conductor, various modifications were considered to inhibit the galloping instability. The chosen solution was to wrap the conductor in PVC tape. The critical Reynolds number was shifted to a slightly higher value, the drop in drag coefficient was reduced and the magnitude of the lift coefficient was greatly reduced (Counihan 1963, Sewell and Taylor 1961). Data are available for very few cable-wind angles, so again rigorous application of the generalised galloping analysis is not viable. However, for zero yaw, the drag-force/velocity curve did not have a negative slope (Sewell and Taylor 1961) and for 15° yaw the force coefficients are similar to those for the cable with 18 outer stands (Counihan 1963), so it seems reasonable to assume that the wrapped cable is also aerodynamically stable. The maximum magnitude of the lift coefficient actually occurs above the critical Reynolds number range, but the magnitude continues to increase with increasing Reynolds number, so $C_L \cdot \partial C_L / \partial Re$ is positive and the cable is not unstable.

The alternative modification of adding four additional strands on the outside of the cable, wound against the lay of the exposed strands, had similar effect to the PVC wrapping, for zero or 10° yaw (Sewell and Taylor 1961), which, from the limited data available, implies that such a cable would not be unstable. One or two additional strands only had a minor effect, implying that they would not prevent the galloping instability.

It seems the only other data in the literature of lift forces on yawed/inclined cables or cylinders in the critical Reynolds number range are from tests made for bridge stay-cables. The galloping behaviour of yawed/inclined smooth circular cylinders has been considered previously (Macdonald and Larose 2006, 2008a, 2008b). Similar independent tests have been undertaken on cables with helical fillets and with a dimpled surface, as well as with a smooth surface (Poulin and Larsen 2007). Galloping analysis yielded reasonably comparable results between the two sets of wind tunnel data for the smooth surface (Symes and Macdonald 2006). For the other surface finishes no galloping was predicted, although it appears all the tests were in the super-critical range.

It is also worth noting that critical Reynolds number effects could be relevant to galloping of other electricity cables, such as iced conductors. Furthermore, it has recently been identified on an overhead test line covered with an aerodynamically unstable D-section, that the most critical wind direction for galloping is not necessarily normal to the line (Van Dyke and Laneville 2008), as is normally assumed. This requires three-dimensional effects to be considered, which are covered by the proposed generalised galloping analysis.

6. Conclusions

The original wind tunnel data for the Severn Crossing Conductor have been used together with the new generalised quasi-steady galloping formulation to predict the wind conditions for large amplitude vibrations to occur. Good agreement with the site observations has been achieved. Time

history analysis, also fundamentally based on quasi-steady theory, predicted vibration amplitudes in excess of 5m in the first anti-symmetric mode pair, which could be sufficient to cause flashover, and again agrees remarkably well with the site observations.

The good agreement supports the assumption that the aerodynamic loads can be treated as quasi-steady, taking proper account of the three-dimensional geometry and critical Reynolds number effects. In particular, there is evidence that the variation of the static force coefficients with Reynolds number is important, so should be included in the analysis, at least for stranded cables at high reduced velocities.

The analysis demonstrates that for certain cable geometries, galloping of single conductors can occur even in the absence of ice or rain, particularly in skew winds. The driving factors are sufficiently negative $\partial C_D/\partial Re$, causing along-wind vibrations, or sufficiently negative $C_L \cdot \partial C_L/\partial Re$ (i.e. decreasing magnitude of lift with increasing Reynolds number), causing vibrations in an inclined plane (or ellipse). The latter occurs at the upper end of the critical Reynolds number range, for stranded cables in skew winds, and was the major cause of large vibrations of the Severn Crossing Conductor. However, from the limited available data, it appears that galloping of stranded cables due to critical Reynolds number effects is unlikely to be a problem for cables with 24 or fewer circular outer strands.

The generalised galloping formulation provides a common framework for analysing dry inclined cable galloping and galloping of stranded cables in skew winds. When variation of the force coefficients with angle of attack are included, it also covers the classical cases of Den Hartog galloping and conventional quasi-steady aerodynamic damping (Macdonald and Larose 2006, 2008a). The method can be applied to any cable geometry, although it is currently limited by the availability of suitable data of static force coefficients, particularly for lift on yawed/inclined cables in the critical Reynolds number range.

Acknowledgements

Kevin Cooper of the National Research Council of Canada is acknowledged for suggesting this study. The first author is supported by an EPSRC Advanced Research Fellowship.

References

- Carassale, L., Freda, A. and Piccardo, G. (2005), "Aeroelastic forces on yawed circular cylinders: Quasi-steady modeling and aerodynamic instability", *Wind Struct.*, **8**(5), 373-388.
- Counihan, J. (1963), "Lift and drag measurements on stranded cables", Imperial College of Science and Technology, Aeronautics Department, Report No. 117.
- Davis, D. A., Richards, D. J. W. and Scriven, R. A. (1963), "Investigation of conductor oscillation on the 275kV crossing over the Rivers Severn and Wye", *Proc. Institution of Electrical Engineers*, **110**(1), 205-219.
- Den Hartog, J. P. (1956), *Mechanical Vibrations* (4th Ed.), McGraw-Hill, New York.
- ESDU (1986), "Mean forces, pressures and flow field velocities for circular cylindrical structures: Single cylinder with two-dimensional flow", Engineering Sciences Data Unit, Data Item 80025, Amendment C.
- Gould, R. W. F. and Lawes, J. A. (1960), "Tests in the compressed-air tunnel on a large diameter stranded cable for the central electricity authority", National Physical Laboratory, Report No. NPL/Aero/412.
- Irvine, H. M. (1981), *Cable Structures*, MIT Press, Cambridge, Massachusetts, USA.
- Jones, K. F. (1992), "Coupled vertical and horizontal galloping", *ASCE J. Eng. Mech.*, **118**(1), 92-107.
- Lilien, J. L., Erpicum, M. and Wolfs, M. (1998), "Overhead line galloping. Field experience during one event in Belgium on last February 13th, 1997" *8th Int. Conf. Atmospheric Icing of Structures*, Reykjavik, Iceland, June

- 1998, pp. 293-299.
- Macdonald, J. H. G. and Larose, G. L. (2006), "A unified approach to aerodynamic damping and drag/lift instabilities, and its application to dry inclined cable galloping", *J. Fluids Struct.*, **22**(2), 229-252.
- Macdonald, J. H. G. and Larose, G. L. (2008a), "Two-degree-of-freedom inclined cable galloping – Part 1: General formulation and solution for perfectly tuned system", *J. Wind Eng. Ind. Aerodyn.*, **96**(3), 291-307.
- Macdonald, J. H. G. and Larose, G. L. (2008b), "Two-degree-of-freedom inclined cable galloping – Part 2: Analysis and prevention for arbitrary frequency ratio", *J. Wind Eng. Ind. Aerodyn.*, **96**(3), 308-326.
- Mathworks Inc. (2005), *MATLAB 7.1*, Massachusetts, USA.
- Nebres, J. V. and Batill, S. M. (1992), "Flow about cylinders with helical surface protrusions", *30th Aerospace Sciences Meeting & Exhibit*, Reno, NV, USA, 6-9 January, AIAA-92-0540.
- Nebres, J., Batill, S. and Nelson, R. (1993), "Flow about yawed, stranded cables", *Experiments in Fluids*, **14**, 49-58.
- Poulin, S. and Larsen, A. (2007), "Drag loading of circular cylinders inclined in the along-wind direction", *J. Wind Eng. Ind. Aerodyn.*, **95**(9-11), 1350-1363.
- Richards, D. J. W. (1963), "Aerodynamic properties of the severn crossing conductor", *Conf. Wind Effects on Buildings and Structures*, National Physical Laboratory, Teddington, Middlesex, UK, 26-28 June, Volume II, Paper No. 8, pp. 688-765.
- Sewell, P. and Taylor, N. P. (1961), "The aerodynamic effects of wind on stranded cables", BSc Thesis, University of Bristol, Department of Aeronautical Engineering, Report No. 58.
- Simpson, A. (1965), "Aerodynamic instability of long-span transmission lines", *Proc. Institution of Electrical Engineers: Power*, **112**(2), 315-324.
- Simpson A. (1983), "Wind-induced vibration of overhead power transmission lines", *Science Progress, Oxford*, **68**, 285-308.
- Symes, J. A. and Macdonald, J. H. G. (2006), "Comparison of quasi-steady "dry-galloping" analysis of inclined cables using two sets of wind tunnel data", *Symp. Mechanics of Slender Structures*, Northampton, UK, 28-29 Sept., Paper No. 17.
- Symes, J. A. and Macdonald, J. H. G. (2007), "The effects of small-scale wind turbulence on dry inclined cable galloping", *12th Int. Conf. Wind Engineering*, Cairns, Australia, 2-6 July, Vol.1, pp.183-190.
- Van Dyke, P. and Laneville, A. (2008), "Galloping of a single conductor covered with a D-section on a high-voltage overhead test line", *J. Wind Eng. Ind. Aerodyn.*, **96**(6-7), 1141-1151.